HUMAN, EARTH AND FUTURE
Ital Publication

ISSN: 2785-2997

Available online at www.HEFJournal.org

Journal of
Human, Earth, and Future

Vol. 3, No. 1, March, 2022

Modeling the Semivariogram of Climatic Scenario around Rivers by Using Stream Network Mapping and Hydrological Indicator

L. Omolayo Agashua [1], B. Dorcas Oluyemi-Ayibiowu [1], N. Isioma Ihimekpen [2], E. Christopher Igibah [2*]

[1] *Department of Civil Engineering, Federal University of Technology Akure, Ondo State, Nigeria*

[2] *Department of Civil Engineering, University of Benin, Edo State, Nigeria*

Received 06 January 2022; Revised 27 February 2022; Accepted 28 February 2022; Published 01 March 2022

Abstract

Precipitation erosivity propels detrimental hydrological happenings with substantial eco-friendly and socio-economic influences. The conception of the precipitation-vegetation interface is very vital for implementing acclimatization and mitigation techniques for terrestrial bionetworks. Numerous investigations have reconnoitered the spatial correlation of precipitation-vegetation context along the season-precipitation quantity gradient. Here, comprehensive scrutiny of spatio-temporal patterns of climatology-vegetation response to seasonal variability incongruities in River Ikpoba, southern Nigeria, using principal component scrutiny (PCS), semivariogram, cross-validation statistics, spatial distribution mapping, and hydrological indicators for multi-source climatic datasets for pre-impact flow (1913–1966) and post-impact flow (1967–2022). PCS outcomes reveal seven PCs whose eigenvalues were greater than one were hauled out of the twenty-five variables. The River Ikpoba water quality variables displayed a moderately strong rate of spatial reliance, which made it possible to create the spatial distribution map for the carefully chosen water quality variables. Results from further scrutiny of the river Ikpoba flow duration curve show the highest flow rate value between 900–1000cms for the month of October. The post-impact flow's highest value was 65cms in 2008, whereas the pre-impact flow was 64cms. Likewise, 90 days' minimum highest flow rate was 250cms, 30 days was 1180cms, 7 days was 105cms, and 1 day was 105cms. Whereas the maximum for 1 day was 7200cms, 3 days' value was 6400cms and 7 days' was 4500cms. This indicates that as the day progressed, the flow rate was increasing for a consecutive 30 days at a low flow rate, but at 90 days it declined. As the day progresses, the values for the maximum value decrease.

Keywords: Distribution Mapping; Impact Flow; Spatial Reliance; Geostatistical; Contagions; Hydrological Indicator; River.

1. Introduction

There is no doubt that climate changeability has given rise to harsh meteorological circumstances and has uninterruptedly disturbed the flow pattern of seas, rivers, and oceans together with the quality of surface water, particularly rivers and streams [1, 2]. With the initiation of more flooding or overflowing and famines, warmer air is produced and excessive water content is held, which in turn makes precipitation styles extreme [3, 4]. Streams, rivers, and lakes, which are fundamental resources for farming or agribusiness, industry, and companies and also a source of drinking and household water for people and animals, have been disparagingly influenced by climatic-changeability dynamics [5, 6]. Freshwater ecosystems around the globe are already down due to disproportionate pressure from drainage, abstraction, dredging, blockading, contamination, silting, and bellicose species [7-9]. Climate changeability only aggravates the problem, even making it worse. Dissipations of drought and overflowing or flooding will become

* Corresponding author: Igibahchrist1@gmail.com

doi http://dx.doi.org/10. 28991/HEF-2022-03-01-02

more frequent, producing dislodgment of neighborhoods and disputes arising from land tussles [10, 11]. Because billions of people rely on these glaciers for household and drinking water [6, 7], hygiene, farming, and hydroelectric power, the impact on these people is only going to get worse [12–14]. Climate changeability has also resulted in widespread temperature increases, which have serious consequences for water supplies and bionetwork functions, as well as health risks for those living in coastal zones [15, 16]. Also, there is intermediate action, irreparable changes in the activities of the ocean and climate structure with key impacts on the weather. These effects will have an impact on the basic necessities of life – good health, food, water, and shelter – for billions of people, and the needier and disadvantaged people living in poorer countries will be disproportionately affected [17, 18]. This triggers philosophical, ethical, and justice matters, given that these people have principally slightly contributed to the causes of comprehensive climate change, particularly the emanation of greenhouse gases, and their scarcity of resources methods that make them the least competent to tackle the effects of climatological change [19-21].

2. Materials and Methods

2.1. Description of Study Region

The Ikpoba River is a fourth-order stream situated within the rainforest belt of Edo District, south-south Nigeria. The river rises from the Ishian Plateau in the arctic part and flows in a south-westerly direction in a precipitously incised valley and via sandy regions before passing through Benin Municipality and joining the Osiomo Stream. Edo State lies roughly between latitudes 05º44' N and 07º34' N, as well as longitudes 06º 04' E and 06º 43' E. Edo State has a tropical climate categorized by two distinct seasons: the wet and dry seasons (Table 1). The wet or humid season occurs between April and October, with a break in August and an average rainfall ranging from one hundred and fifty centimeters (150cm) in the extreme arctic of the state to 250 cm in the south. The arid season lasts from November to April with a cold harmattan spell between December and January (Okonofua et al. (2019) [11]; Benka-Coker and Ojior (2015) [18]; Ilaboya et al. (2014) [16]; Ekhaise and Anyasi (2011) [22]). Techniques for water quality assessment are displayed in Table 2. Twenty-four (24) samples of water were collected at a distance of 10 meters apart along the stretch of the river during the humid season (July, 2021) and dry season (November, 2020), respectively. Water samplings were stored in two hundred and fifty millimeter (250 ml) sampling bottles and then placed in the ice box and then analyzed [23].

Table 1. River Ikpoba and activities around its settlement

N/A	Activities	Description	Photograph	Effects
1	Industrial effluence	Discharged into the river at various points		Pollution impact
2	Water from drainage channels	Discharged into the river at various points		Effluent impact
3	Flooding	-		Catastrophe effect
4	Abattoir	-		Pollution though numerous locality rely on the river for their source of water supply.
5	Religious Activities	-		Such as water baptism by Christianity.
6	Agricultural activities	-		A non-efficient overgrow with crops.

2.2. Fitting and Testing of Semivariogram

Four semivariogram models, namely; Circular, Spherical, Stable and Exponential were fitted for each of the seven critical water quality parameters used for geo-statistical analysis. Figures 5a to 5f (See section "3.5. Generation of Spatial Distribution Map") displays the outcome of the semivariogram models for total suspended solids (TSS), nitrate, zinc, copper, alkalinity and turbidity plus the corresponding values of nugget (the inconsistency in the field data that cannot be clarified by distance among the observations), major range (denotes the distance at which two observations are disparate, distinct/independent) and sill (the semi-variance at which the leveling occur. The end point of range is the start off point of sill, and partial sill is the discrepancy between the sill as well as the nugget).

2.3. Assessment of Climate Change Impact on Hydrological Indicators

The index engaged for scrutiny of monthly flow regimen was created by Haghighi and Kløve, (2015) [24]. This deliberates on three vital physiognomies of monthly flow which comprising of timing of intra-annual flow, magnitude, and variability. These features are influenced either by climate or land use revolution. Hence, Variation Impact Factor (VIF), Magnitude Impact Factor (MIF), as well as Timing Impact Factor (TIF) are propositioned to quantify these vicissitudes.

Magnitude Impact Factor (MIF)

The magnitude impact factor (MIF) was computed via the mass balance equations displayed as follows;

$$MIF_1 = \frac{AOF}{AIF} \tag{1}$$

$$MIF_2 = \frac{AF_{post}}{AF_{pre}} \tag{2}$$

If the assessed value of MIF is above 1, thenceforth a revolution equation will be engaged as follows;

$$MIF_{final\ \mathrm{value}} = 1 - \left|1 - MIF_{calculatedv\ \mathrm{value}}\right| \tag{3}$$

Besides, Haghighi and Kløve (2015) [24] also advocate using the MIF2 technique for the evaluation of flow regime alteration owing to climate change.

Where; AOF as well as AIF are the annual out-flow and in-flow from the river, and both AF_{post} as well as AF_{pre} are the peak annual flow for arid and wet seasons.

Table 2. Water quality features and measurement techniques

No.	Variables	Acronym	Unit	Measurement Site	Techniques
		Microbiological variables			
1	Total Dissolve Solid	TDS	mg/l	Gravimetric	In the Lab
2	Temperature	T	^0C	Thermometer	On site
3	Total Suspended Solid	TSS	mg/l	Gravimetric	In the Lab
4	Electrical Conductivity	EC	mg/l	Multi-parameters meter	On site
5	Turbidity	Turb	NTU	Turbidity meter	In the Lab
6	Hydrogen ion concentration	pH	-	pH Meter	On site
7	Dissolved Oxygen	DO	mg/l	Lutron5509DOmeter	On site
8	Carbonate Hardness	CH	mg/s	EDTA Titration	In the Lab
9	Chloride	Cl^-	mg/l	Argentometric Titration	In the Lab
10	Alkalinity	A	mg/l	Titration	In the Lab
11	Bacterial Oxygen Demand	BOD	mg/l	Winkler & incubator	In the Lab
12	Chemical Oxygen Demand	COD	mg/l	Reflux K2C-207	In the Lab
13	Sodium	Na+	mg/l		In the Lab
		Heavy metals variables			
14	Cadmium	Cd	mg/l	UNICAM 969 AAS	In the Lab
15	Lead	Pb	mg/l	UNICAM 969 AAS	In the Lab
16	Zinc	Zn	mg/l	UNICAM 969 AAS	In the Lab
17	Copper	Cu	mg/l	UNICAM 969 AAS	In the Lab
18	Iron	fe	mg/l	UNICAM 969 AAS	In the Lab
19	Nickel	Ni	mg/l	UNICAM 969 AAS	In the Lab

Anions variables					
20	Nitrite	NO_2	mg/l	UV obvious spectrophotometer	In the Lab
21	Phosphate	P	mg/l	UV obvious spectrophotometer	In the Lab
22	Calcium	Ca	mg/l	UV obvious spectrophotometer	In the Lab
23	Sulphate	SO_4	mg/l	UV obvious spectrophotometer	In the Lab
24	Nitrate	NO_3	mg/l	UV obvious spectrophotometer	In the Lab

Variability Impact Factor (VIF)

The variability impact factor (VIF) is assessed as: $VIF = \frac{50 - 0.5(I_{RR})}{100}$. (4)

Where; I_{RR} denotes relative variation in RRI, which is displayed as: $I_{RR} = \frac{|RRI_{pre} - RRI_{pos}|}{RRI_{pre} * 100}$. (5)

Where; RRI_{pre} as well as RRI_{pos} are the RRI (River or stream regime index) in the pre- and post-periods respectively. River or stream Regime Index (RRI) is for determining the intra-annual flow regime of rivers that depends on the changeability in yearly flow hydrograph. Likewise, to estimate RRI_{pre} and RRI_{pos} index, the hydrograph for both humid and dry seasons must gotten and the magnitude of variation in the peak flow was then assessed.

Timing Impact Factor (TIF)

The flow timing impact factor (TIF) take into consideration changes of maximum timing, minimum timing as well as timing of the 50% value of the ejection cumulative density function (cdf 50%, explicitly; the spot when cumulative discharge attains the median):

$$TIF = \frac{(50 - 0.274 * TF)}{100} \quad (6)$$

$$TF = \frac{(|DT_{\max}| + |DT_{median}| + |DT_{\min}|)}{3} \quad (7)$$

Where DT_{max} as well as DT_{min} are the time transference in monthly minimum and maximum ejection. Similarly, DT_{median} is the time transference in cdf50% timing value. Centered on these three impacts, an amalgamated river impact factor (RI) utilized the techniques created by Haghighi and Kløve (2015) [24] and listed as:

$$RI = MIF * (TIF + VIF) \quad (8)$$

where; RI is the river or stream indicator, rangings from 0 to 1, 1 denotes natural stream or river flow scenario and 0 epitomizes completely transformed river. Also the stream impact factor is further sectioned into numerous types based on the range of variation given in Table 3.

Table 3. Hydrological indicators and river impact

Threshold Exceedance	Class of Impacts	Range of River Impact (RI)	Class of Impact
0	No	0.8-1	Low
1-20	Low	0.6-0.8	Incipient
21-40	Medium	0.4-0.6	Moderate
41-60	High	0.2-0.4	Severe
		0-0.2	Drastic

3. Results and Discussion

3.1. Impacts of Principal Component Scrutiny on River Ikpoba

To establish the key contagion factors that inspired every identified stream region verified in Tables 4 and 5, besides visually displayed in Figure 1, factor scrutiny was engaged on consistent log altered data sets for contagion precincts. Factor analysis created seven variance factors (PCs) for contamination precincts from the 25 parameters.

Table 4. Result of horizontal decentralization of the component matrix

Variables and their values						
PC1 (24.0%)	**PC2 (20.0%)**	**PC3 (20.0%)**	**PC4 (12.0%)**	**PC5 (8.0%)**	**PC6 (8.0%)**	**PC7 (8.0%)**
Sulphate =0.79	Nitrate = 0.79	Lead =0.75	DO =0.13	Carbonate =0.70	pH =0.72	Turbidity =0.72
TSS= 0.80	EC =0.63	Zinc =0.79	Nitrite =0.93	Alkalinity =0.83	Copper =0.74	Iron =0.31
Cadmium =0.76	TDS =0.56	Chloride =0.57	Phosphate =0.79			
Calcium =0.76	Sodium =0.74	Nickel =0.74				
Manganese =0.59	THC =0.68	COD =0.54				
TCC =0.7						

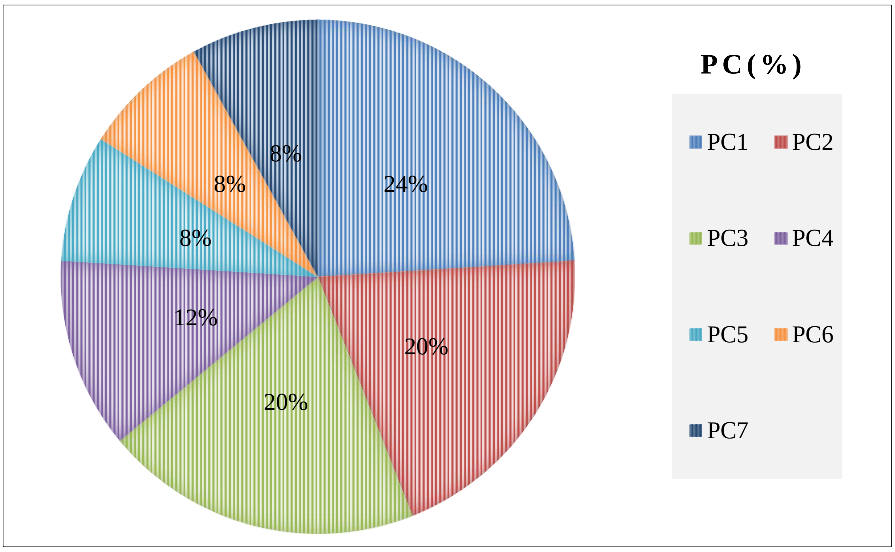

Figure 1. Percentages of Rotated Component Matrix PC

Principal component Scrutiny (PCS) aids in the clarification of acculturated multi-dimensional data for an enriched grasping of water attribute. Seven PC whose eigenvalues was greater than one were haul out from the twenty-five variables. The first principal component PC1, has high assenting loading on TSS (+0.80), sulphate (+0.79), cadmium (+0.78), calcium (+0.76), TCC (+0.70) and Manganese (+0.59) as displayed in Table 4.Excessive total suspended solids (TSS) in drinking, domestic or wastewater may have effects on both environmental and human health. While on water quality, high TSS might lessening water's natural dissolved oxygen (DO) levels and enhance water temperature. Suspended solids in rivers are frequently due to natural reasons, such as natural solids comprise organic substances like algae, and inorganic substances (silt and sediment).

Some algae like phytoplankton are consistently occurs specifically in both saltwater as well as freshwater origins [4, 25]. Especially when these organisms die they released organic substance into the water, decreasing water's oxygen quantities and increasing TSS levels. Similarly, Cadmium occur in the river water owing to corrosion of galvanized plumbing in consort with industrial waste and certain fertilizers contagions. Naturally cadmium ensues in lead, copper ores, zinc, coal, fossil fuels, shales and discharge in the course of volcanic deed [3, 5]. Sulphate denotes the physicochemical, leaking of agrarian wastes into the river, excretion, wastewaters from household activities. Also excessive values can cause accidental leaks when the alkalinity of the river water is little. Likewise, TCC was strongly correlated with built-up sewage and wastewater contagion origins along the river. Natural effluence is influenced via seasonal vicissitudes, for instance, the contamination impact of weathering and soil erosion on river water attribute throughout rainy season [8]. Manganese may occur naturally or through microbial factor contagions sources for instances built-up and industrial contagions, agricultural deeds etcetra. Furthermore, PC2 have huge loadings on nitrate (+0.79), sodium (0.74), THC (+0.68), and TDS (+0.56). The greater loading of sodium and nitrate may be credited to the agro-sources like composts and animal waste, eroding of plagioclase feldspars, and suspension of lithoigenic substances. More so, the occurrence of Nitrate might be owing to agrarian runoff from cultured fields via rain erosion deeds. Other origins of nitrates in the lakes and streams comprises of septic structures, animal fodder-lots, agricultural composts, garbage landfills, bottom–nurturing irregular fish like carp that can incite bottom residues, and in turn emancipating nitrate back into the river [20, 21].

Table 5. The principal component of River Ikpoba Parameters via Rotated component matrix

Variables	Components						
	PC1	PC2	PC3	PC4	PC5	PC6	PC7
pH	-0.139	-0.043	-0.002	-0.05	0.152	**0.719**	0.163
Nitrate	0.33	**0.785**	0.173	-0.023	0.08	0.293	-0.058
EC	0.31	0.63	-0.139	-0.002	0.296	-0.038	0.344
Turbidity	-0.206	0.085	-0.106	-0.143	-0.213	0.061	**0.72**
DO	-0.366	-0.678	-0.011	**0.127**	-0.024	-0.3	-0.211
TDS	0.059	**0.558**	-0.238	-0.245	0.164	-0.276	0.312
Sodium	0.49	**0.741**	0.075	0.124	0.138	0.014	-0.044
Lead	0.168	0.189	**0.745**	-0.278	0.003	0.102	-0.259
Sulphate	**0.788**	0.389	0.134	0.002	0.08	0.113	-0.25
Zinc	0.037	0.029	**0.793**	0.281	-0.033	0.2	-0.188
Copper	0.235	0.125	0.048	0.089	-0.117	**0.738**	-0.168
Chloride	0.199	0.115	**0.57**	0.522	-0.342	0.03	-0.147
Iron	0.06	-0.119	0.005	-0.163	-0.793	-0.217	**0.306**
Carbonate	0.366	0.384	-0.096	-0.233	**0.699**	0.099	-0.011
TSS	**0.795**	0.362	0.087	0.012	0.14	0.031	-0.124
Nitrite	-0.061	-0.023	0.025	**0.934**	-0.027	-0.126	-0.122
Cadmium	**0.777**	0.191	0.009	0.049	0.077	-0.074	-0.125
Nickel	-0.128	-0.16	**0.736**	-0.135	0.175	-0.277	0.377
THC	0.195	**0.678**	0.066	0.19	0.023	-0.111	-0.151
Phosphate	0.31	0.108	-0.039	**0.793**	0.026	0.264	-0.036
Alkalinity	0.314	0.061	0.147	-0.088	**0.832**	-0.195	0.056
Calcium	**0.757**	0.477	-0.027	0.077	0.08	-0.114	-0.143
Manganese	**0.586**	0.04	0.531	0.035	0.281	-0.018	0.171
Total coliform count	**0.7**	0.1	0.058	0.246	0.073	0.264	0.239
COD	0.082	-0.484	**0.537**	0.485	0.023	-0.177	0.04

Bold values specify strong loadings.

Moreover, TDS function as a prevalent pointer of adulterated waters, besides divulges the outward sources for the suspension of rocks by river infusing directly via the soil bearing secondary gypsum [1]. It means reliant of the chemical nature of the river and the solubility of the aquifer substances via which the river water is flows. Ogwueleka and Igibah (2020) [5] professed that excessive TDS occur via sediment suspension, ion exchange, evaporation, and rainwater. Unmistakably, PC2 connotes the impact of contagion from chemical stimulants /fertilizers or mineral dissolution. This specifies that the features of river water in the investigation zone are significantly reliant on the sources. Additionally, PC3 own extreme positive loading on zinc (+0.79), lead (+0.75), nickel (+0.74) and COD (+0.54). Excessive level of zinc is frequently connected with greater absorptions of other metals vividly, lead and cadmium. The majority of zinc is initiated into river via artificial pathways (by-products of steel manufacturing, mine tailing, burning of waste substances, stimulants and wood preservations that have zinc). When the metals are triggered from the ore fluids via various techniques for examples pH variation, cooling, and mixing with other fluids, then zinc react with the river water and discharges hydrogen that oxidizes with oxygen explosively, which can in turn add an undesirable flavour to water. Whereas lead ensue where water has excessive acidity or small quantity that oxidizes [12, 22]. For nickel the natural origins include wind-propelled dust drawn from eroding of rocks as well as soils, forest fires and volcano deeds. Nickel concentrations rest on pH and soil, for instance, nickel tetra carbonyl is river water impenetrable, but is noxious and carcinogenic nonetheless upon ingestion of excessive prescriptions one usually vomits, as a result of swift ejection from the river. Besides, nickel originate from the incineration of waste, sewage and coal, diesel as well as fuel oil. What's more, COD denoted mixed contamination factors (natural as well as organic contagion), and the erosion from highland zones throughout precipitation actions [15, 21]. The positive connection with COD specifies the loading of moderately decayed organic substances from river areas.

Also, PC4 has immense loading on Nitrite (+0.93), Phosphate (+0.79) and DO (+0.13), with simplified variance percentage of 8.0%. Nitrite are ester of nitrous acid or a salt that are naturally or artificially occurrence emanates from stimulants like composts and fertilizers in river. It also symbolizes form of nitrogen which is gotten from numerous diverse forms in aquatic and terrestrial ecologies [6, 13]. More to the point, excessive level of nitrite motivates the sprouted of bacteria when introduced in extreme levels via agrarian runoff, refuse dump, or contagion with human or animal rubbishes. The concentration frequently vacillates and fluctuates with the season and might rise when the river is being nurtured via nitrate-rich aquifers. Under usual water flows, approximately two-thirds of all phosphorus load to seas, oceans and rivers emanates from non-point origins like runoff from grazing land, atmospheric removal and river and sea bank erosion. Meanwhile, strong connection of DO in the low-contagion zone indicated the low level of organic contagion within the region. PC5 have extreme positive loading on alkalinity (+0.83) and carbonate (+0.70). Both Alkalinity and carbonate are interrelated to the water hardness. The carbonate rocks are a substantial source of alkalinity, and their ions are extensively distributed in nature. They could enter the water through built-up landfill leachate, agronomic chemicals, rock weathering, motorway deicers, and irrigation absorption. PC6 also has enormous loadings on copper (+0.74) and pH (+0.72). High quantities of copper may enter the environment via mining, agri-business, manufacturing, operations, built-up wastewater discharges into the rivers, seas and lakes. They frequently found in river systems as a result of anthropogenic origins, human and volcanic deeds, geological sediments, erosion of both rocks as well as soils. pH a substantial water attribute parameter, serves as controlling factor that defines the types of ion available in water and also displays the potency of the river water to react with either alkaline or acidic substances [5, 9, 14].

Similarly, PC7 holds vast loadings on turbidity (+0.72) and iron (+0.31). Excessive turbidity in rivers can be triggered by natural goings-on such as heavy rains, windstorms, snowmelt, and ice scouring. It can also be caused by particles suspended or melted in river water that disseminate light and, in turn, make the river look cloudy or shadowy. Particulate substance comprises of sediment – exclusively clay as well as silt residue, fine carbon-based and inorganic substance, fathomable colored carbon-based composites, algae, other minuscule entities and human deeds in upstream regions. For excessive quantity of iron in the river water samples can ensue from the pump substances and verdigris of conveyance pipes via river water of inconsequential pH value [10, 11].

Persuasively, PC1, PC2, PC3, PC4, PC5, PC6 and PC7 were impacted through extreme values of heavy metals cause by geogenic industrial, agrarian, pharmaceutical, household effluents and atmospheric origins, comparing with current scenario around River Ikpoba in Table 1, which reveals vividly most of catastrophic effects such as industrial effluence, religion deeds, flooding, drainage, riparian activities, fresh water matrices and etcetera. Thus outcome from laboratory scrutiny reflects true pictures of effects around the river.

3.2. Effects of Semivariogram on River Ikpoba Parameters

Table 6 and Figures 2 to 4 displaying Semivariogram model for TSS, Nitrate, Zinc, Copper and Turbidity. Fitted Semivariogram models exhibited in Table 6 and Figures 2 to 4 specified information about the range, nugget and partial sill which is Model variables that were utilized for measuring the rate of spatial reliance of surface water sampling points via distance between them. It also affords the input variables that were applied for the kriging exclamation /interpolation. The result showed that for Nugget; circular model type of Zinc has the highest (44.56), followed by spherical model type of Zinc (39.80) while circular model type of copper recorded the least (20.99). For Major range; All model type of Copper has the highest 10,089.1), followed by all model type of Nitrate (1567.8) whereas all model type of TSS recorded the lowest (1224.01). Similarly, exponential model type of TSS recorded the highest partial sill (58.44). This was followed by spherical model type of TSS (44.49) while stable model type of copper recorded the least value of (22.10). To choose the model that best portrayed every water quality variable, besides to engaged for generating the final prediction mapping, selected goodness of fit statistics created from the cross-validation step were utilized [11, 16].

Table 6. Semivariogram model for TSS, Nitrate, Zinc, Copper and Turbidity

Model Type	TSS			Nitrate			Zinc		
	Nugget	**Major Range**	**Partial Sill**	**Nugget**	**Major Range**	**Partial Sill**	**Nugget**	**Major Range**	**Partial Sill**
Circular	23.456	1224.01	34.67	33.23	1567.8	24.56	44.56	1304.56	32.11
Spherical	22.207	1224.01	44.49	28.97	1567.8	36.07	39.80	1304.56	29.89
Stable	23.106	1224.01	29.77	25.67	1567.8	27.88	38.79	1304.56	30.05
Exponential	25.894	1224.01	58.44	31.45	1567.8	33.56	33.45	1304.56	35.67
	Copper						**Turbidity**		
Circular	20.99	10089.1	31.02				37.68	1500.89	22.13
Spherical	23.11	10089.1	33.56				25.66	1500.89	30.09
Stable	26.55	10089.1	22.10				24.33	1500.89	28.88
Exponential	27.88	10089.1	27.79				33.11	1500.89	29.08

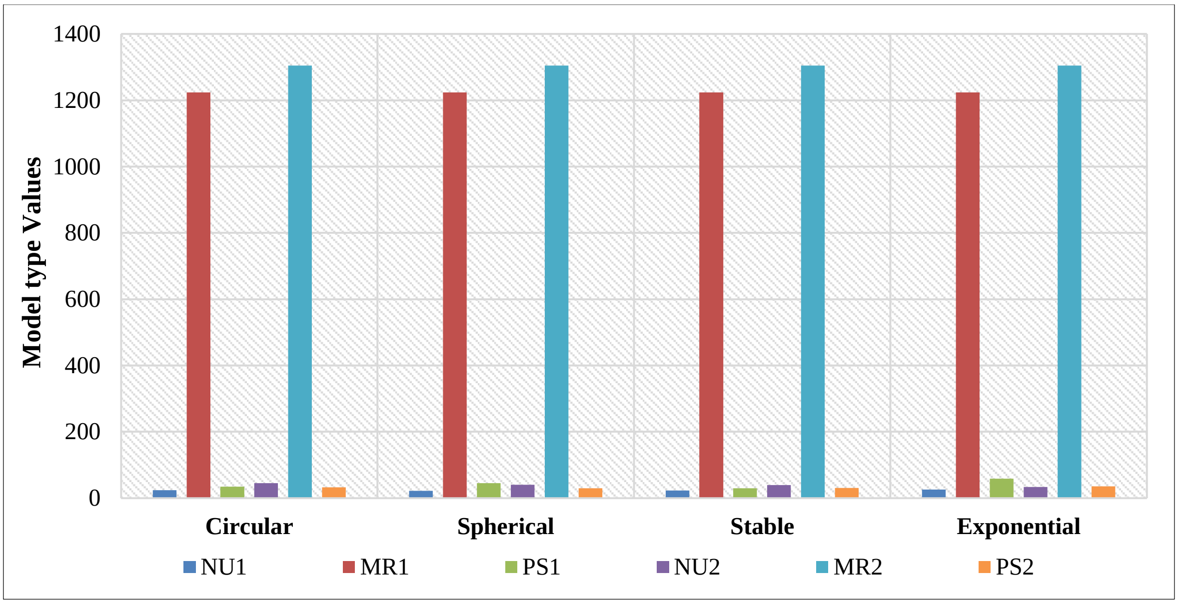

Figure 2. Semivariogram model chart displaying TSS as 1 and Zinc as 2

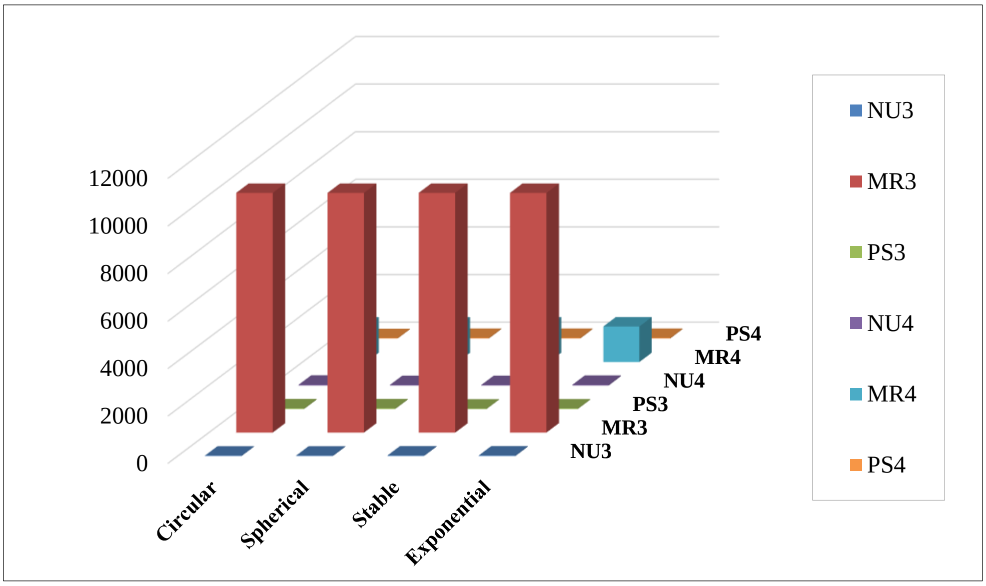

Figure 3. Semivariogram model chart displaying Copper as 3 and Turbidity as 4

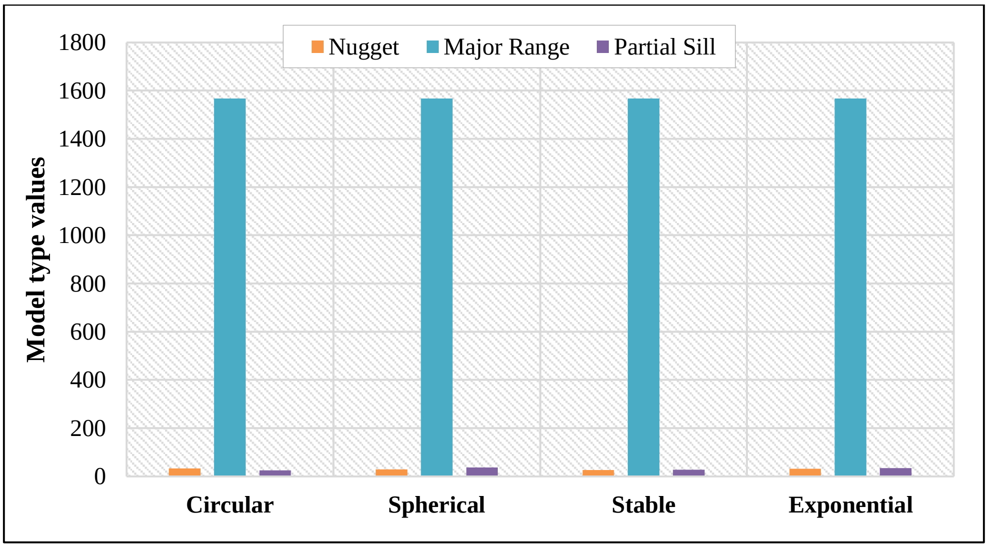

Figure 4. Semivariogram model chart for Turbidity

3.3. Estimation of Cross Validation Statistics

To choice the utmost appropriate model needed to create the final prediction map, nominated goodness of fit statistics, explicitly; Root mean square error (RMSE), Average standard error (ASE), Mean square error (MSE), and Root mean square standardized error (RMSSE) were engaged and the scrutinized values corresponding to the diverse models is exhibited in Table 7.

Table 7. Result of cross validation statistics for TSS, Nitrate, Zinc, Copper and Turbidity

Model Type	RMSE	MSE	RMSSE	ASE	RMSE	MSE	RMSSE	ASE	RMSE	MSE
	TSS				**Nitrate**				**Turbidity**	
Circular	6.828	-0.0061	1.245	5.369	6.811	-0.0045	1.332	5.369	3.256	-0.0035
Spherical	6.944	-0.0029	1.255	5.408	6.902	-0.0029	1.267	5.408	4.056	-0.0045
Stable	4.949	-0.0025	1.255	5.415	3.405	-0.0021	1.201	5.415	2.109	-0.0011
Exponential	6.972	-0.0007	1.241	5.496	6.001	-0.0034	1.247	5.496	3.446	-0.0031
	Zinc				**Copper**				**RMSSE**	**ASE**
Circular	7.890	-0.0061	1.245	5.301	8.092	-0.0067	1.201	5.377	1.098	5.001
Spherical	6.776	-0.0029	1.255	5.447	6.889	-0.0045	1.244	5.477	1.331	5.003
Stable	1.206	-0.0025	1.255	5.422	0.956	-0.0022	1.201	2.422	1.248	2.005
Exponential	6.445	-0.0007	1.241	5.433	6.92	-0.0045	1.211	5.445	1.098	5.444

3.4. Spatial Dependency

After the application of diverse models on every water quality variable, the decisive factor for decide on the best model is that mean homogeneous error must close to 0, root mean square error as well as average standard error must be insignificant and nigh to one another and the root mean square homogenous error must also be close to 1 [12, 17]. Based on the above principle, the stable model was carefully chosen as the best fit model for every designated water quality test variable. Similarly, fitted semivariogram chart was utilized to assess the spatial dependence among the measured sampling points, via the stable model and an abridge Table 8 was produced.

Table 8. Summary table for estimating spatial dependence/ reliance of surface water quality parameters

Parameter	Best Model	Major Range	Nugget (C_n)	Partial Sill	Sill (C)	(C_n/C)	Degree of Spatial Dependency
TSS	Stable	1224.01	23.106	29.77	52.88	0.4370	Strong
Nitrate	Stable	1567.8	25.67	27.88	53.55	0.4794	Strong
Zinc	Stable	1304.56	38.79	30.05	68.84	0.5635	Strong
Copper	Stable	10089.1	26.55	22.10	48.65	0.5457	Strong
Turbidity	Stable	1500.89	24.33	28.88	53.88	0.4516	Strong

The sill (c) is the summation/sum total of nugget as well as partial sill, whereas the ratio of Nugget to Sill was also employed to ascertain the degree of spatial structure (reliance) of water quality variable. The ratio below 25%, specifies that the parameters has strong partial reliance; while between 25% and 75%, displays that the parameters has moderate spatial reliance, and above 75%, the variable indicates only weak or ineffectual spatial reliance. Thus, the outcomes of Table 8 publicised that the River Ikpoba water quality variable showed moderately strong rate of spatial reliance which made it possible to create the spatial distribution map for the carefully chosen water quality variable as demonstrated in Figures 5a to 5f.

3.5. Generation of Spatial Distribution Map

The basic steps invloved in the development of the spatial distribution map of the critical water quality parameters around the study location using kriging interpolation method is presented in Figures 5a to 5f. The spatial distribution map which can be employed to predict the concentration of TSS, Nitrate, Zinc, Copper, Alkalinity and Turbidity within the study area was generated and presented in Figures 5a-f. respectively.

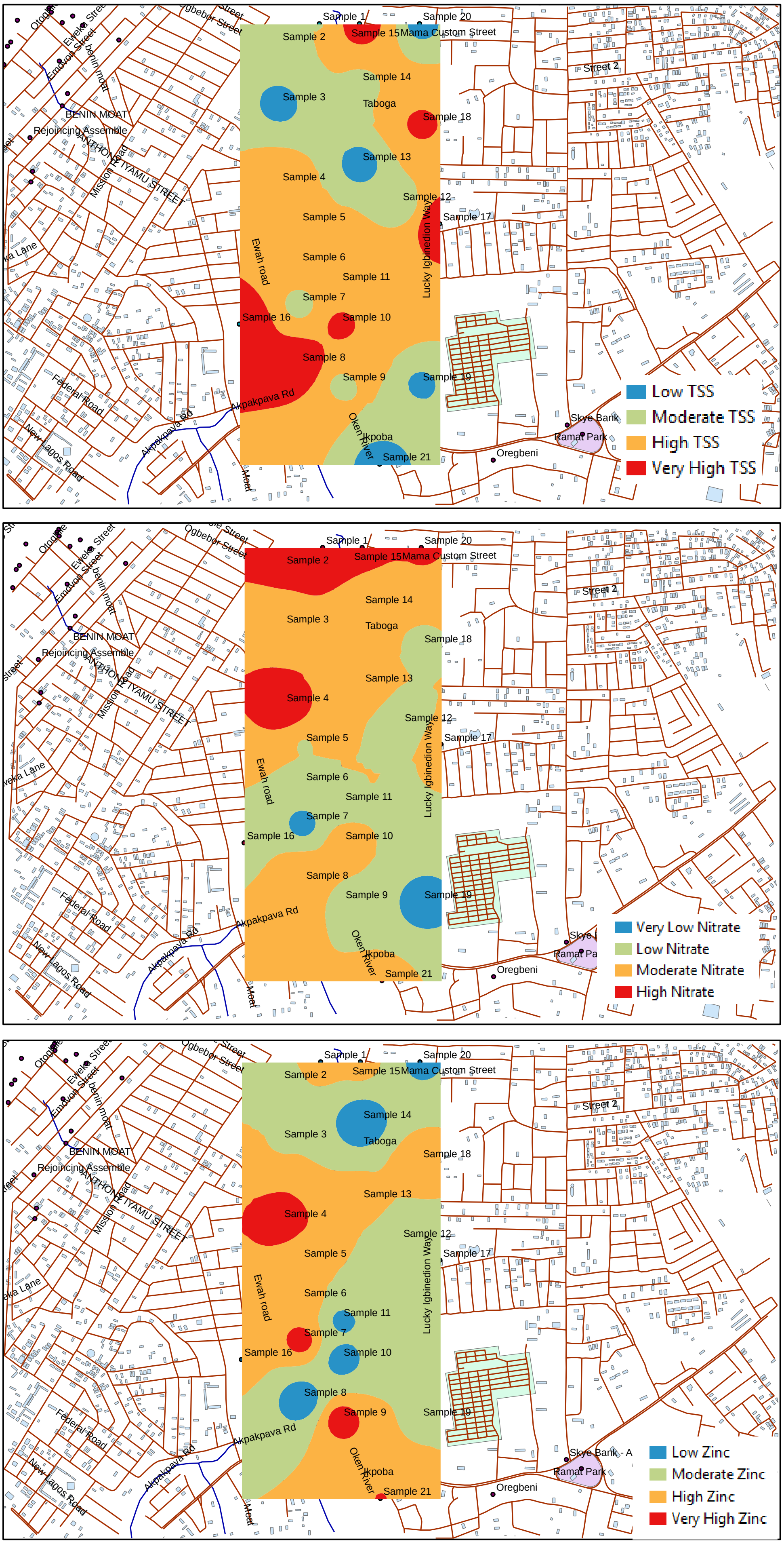
Low TSS
Moderate TSS
High TSS
Very High TSS
Very Low Nitrate
Low Nitrate
Moderate Nitrate
High Nitrate
Low Zinc
Moderate Zinc
High Zinc
Very High Zinc
Sample 1
Sample 2
Sample 3
Sample 4
Sample 5
Sample 6
Sample 7
Sample 8
Sample 9
Sample 10
Sample 11
Sample 12
Sample 13
Sample 14
Sample 15
Sample 16
Sample 17
Sample 18
Sample 19
Sample 20
Sample 21
Mama Custom Street
Taboga
Ewah road
Lucky Igbinedion Way
Akpakpava Rd
Ikpoba
Oregbeni
Skye Bank
Ramat Park
Street 2
BENIN MOAT
Rejoicing Assemble
Mission Road
Federal Road
New Lagos Road
Ogbebor Street

(a)

(b)

(c)

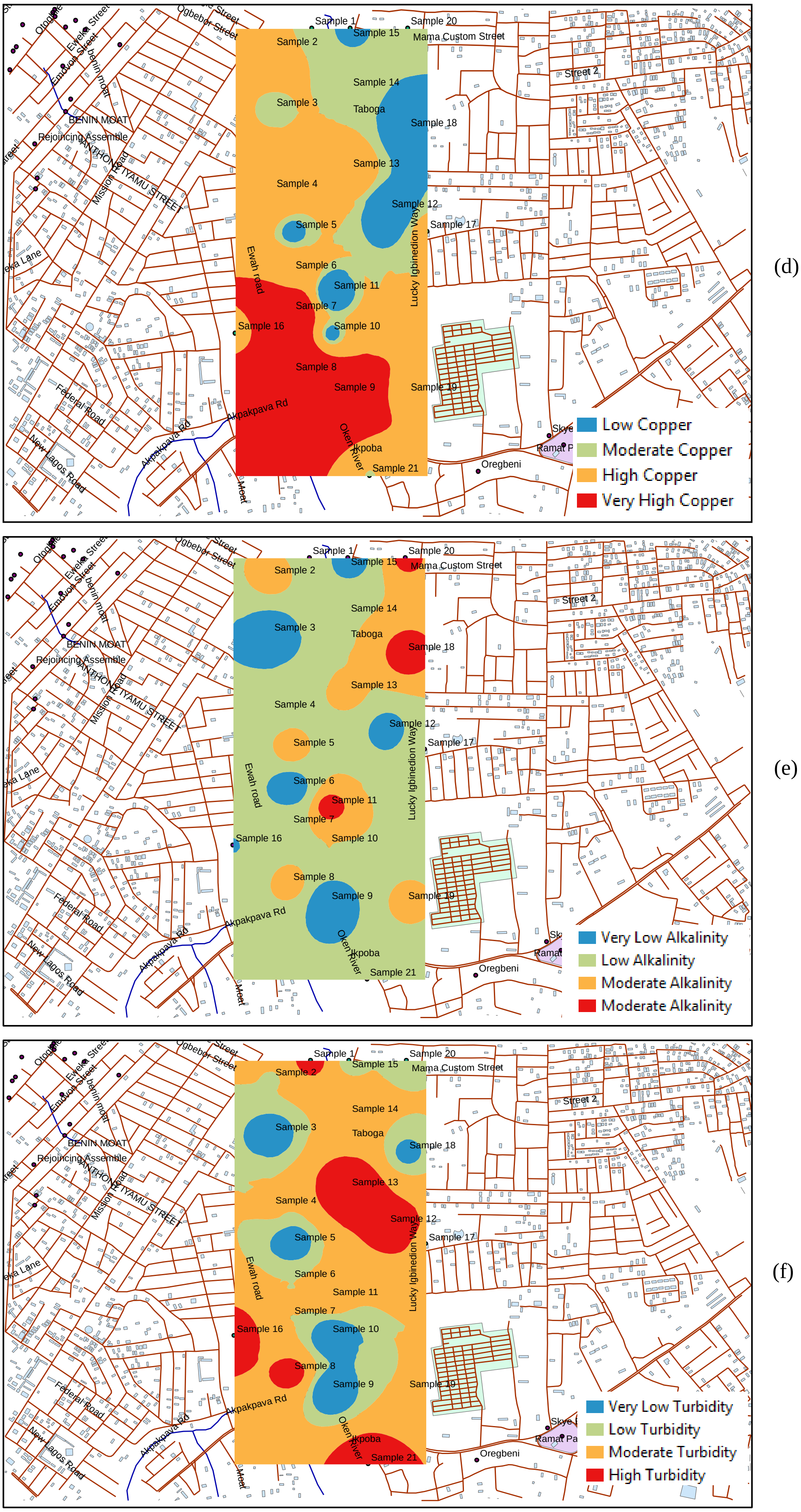

Figure 5. Prediction map along Ikpoba River during Wet Season for; a) TSS, b) Nitrate, c) Zinc, d) Copper, e) Alkalinity, and f) Turbidity

3.6. Impact of Hydrologic Alteration factors on Ikpoba River

Result from Figures 6 to 9 displayed the Hydrology Alteration, flow duration and Peak values of Extreme low flows for pre and post data. During scrutinizing the variation between double time periods, the IHA software assists users to engage the Range of Variability Approach (RVA) as prescribed [26]. From RVA outcome, a positive HA factor indicates an enhanced frequency of values in the category from the pre-impact time to post-impact phase, whereas a negative value signifies that the frequency of values has declined. The HA factors are exhibited in the upper left corner of the 7-days maximum flows of floods graph. In this research, the frequency or rate of recurrence of values in the lower category has improved, whereas the rate of occurrence values in the central and high groupings has diminished. The RVA utilized the pre-development ecological dissimilarity of IHA variable values as a reference point for describing the magnitude to which natural flow regimens have been modified, and enumerates this modification in a series of Hydrologic Alteration factors (HAF). In an RVA scrutiny, the complete range of pre-impact data for every variable is split into three distinct categories (IPCC 2022) [27].

The default technique for non-parametric scrutiny is by dividing the data into three equivalent sets; these are: 0-33rd percentile, 34th-67th percentile, and 68th-100th percentile). The precincts between these classes are displayed on the graph as straight black lines [16]. Then the program calculates the expected rate of recurrence with which the post-effect values of the IHA variables must be within each class, centered on the pre-effect rate of recurrence in the non-parametric default, which was 33.0% of the yearly values in each of the three sets. Then the computation of the regularity with which the post-effect yearly values of IHA variables of 18.0, which essentially lies within every of the three classes. Hydrologic Alteration factor is afterward computed for each of the three classes as - (observed rate of occurrence – anticipated rate of occurrence) / anticipated rate of occurrence.

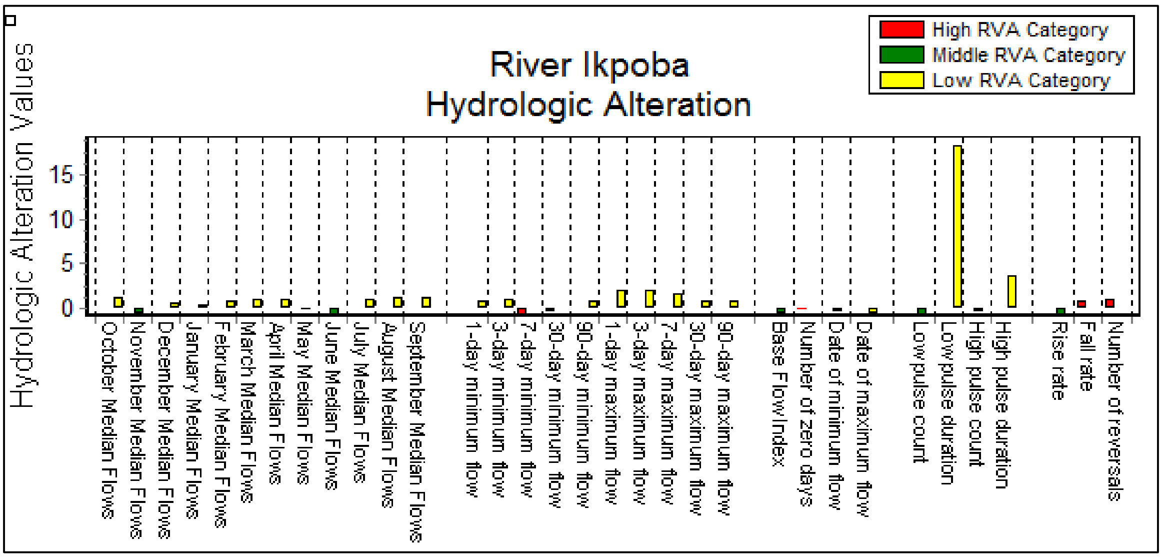

Figure 6. Variation of Hydrology Alteration of River Ikpoba

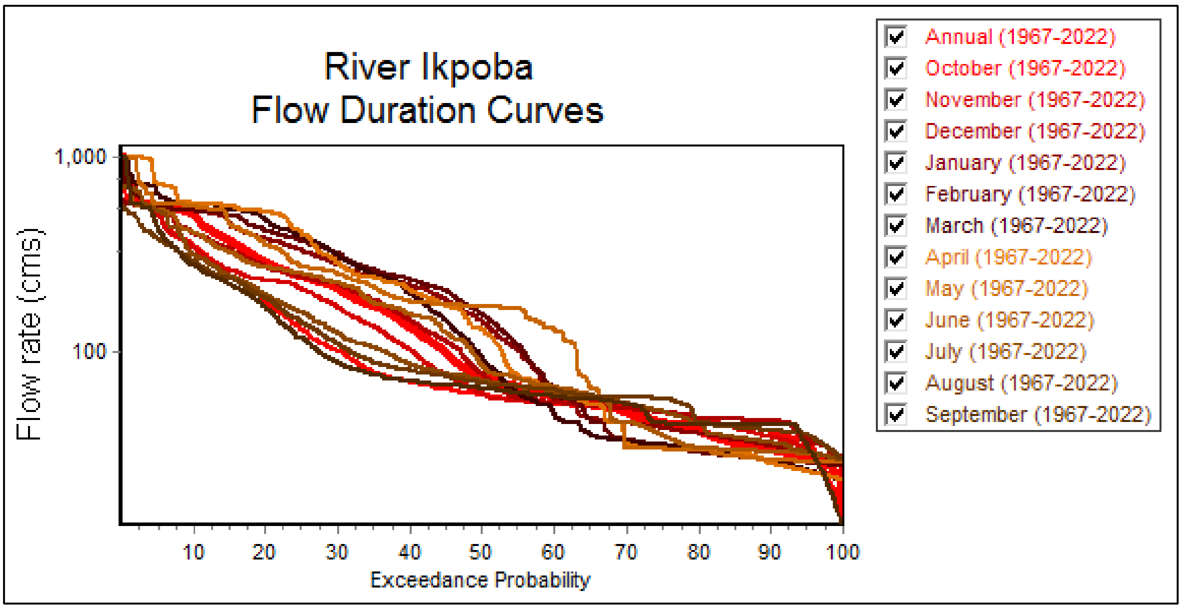

Figure 7. Variation of Flow duration curve

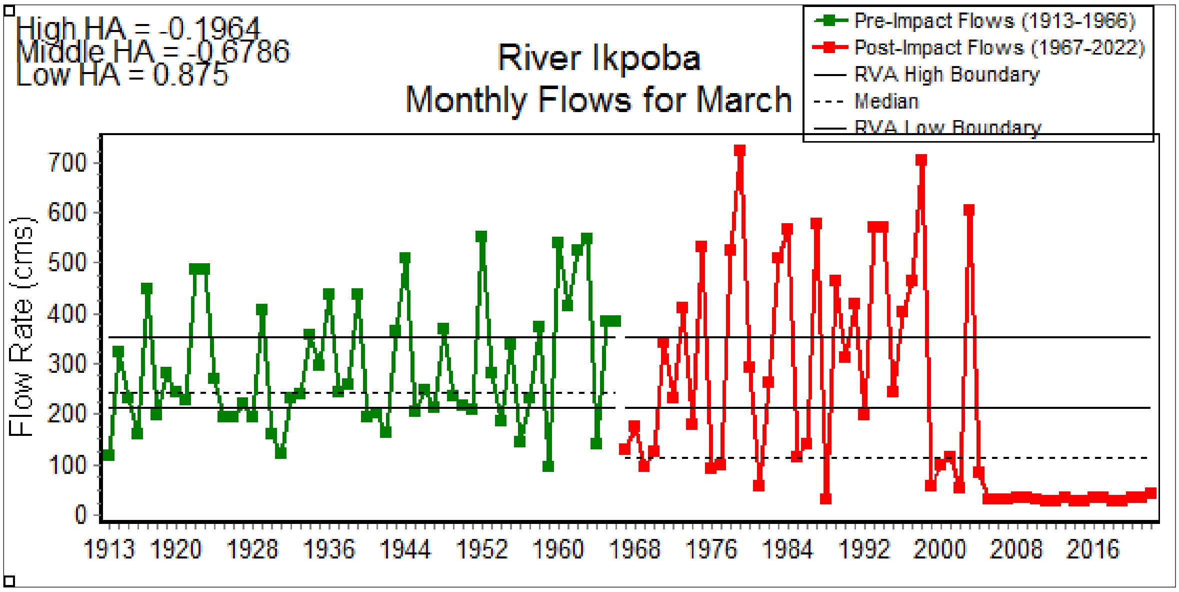

Figure 8. Changeability of River Ikpoba monthly flows for March

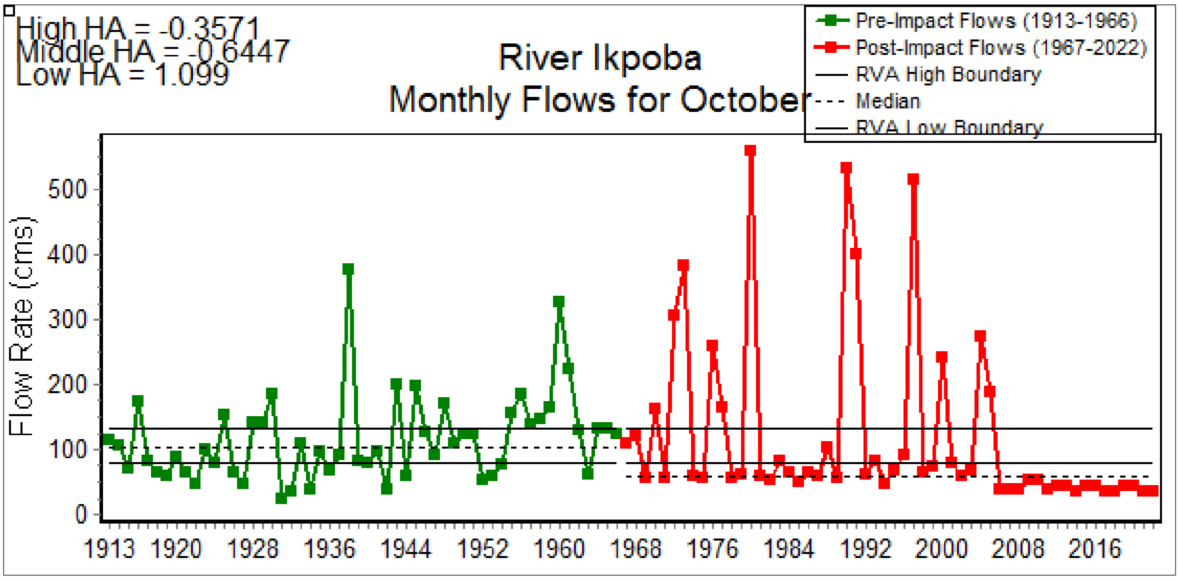

Figure 9. Changeability of River Ikpoba monthly flows for October

Figures 6 to 9 reveal that among the hydrologic alteration high pulse count and high pulse duration of the River Ikpoba has the lowest RVA category of 15, while both December and January fall into the middle RVA category. The flow duration curve shows the highest flow rate value between 900–1000cms for the months of October. The post-impact flow highest value was 65cms in 2008, whereas the pre-impact flow was 64cms. Likewise, 90 days' minimum highest flow rate was 250cms, 30 days was 1180cms, 7 days was 105cms, and 1 day was 105cms. Whereas the maximum for 1 day was 7200cms, 3 days' value was 6400cms and 7 days' was 4500cms. This indicates that as the day progresses, the flow rate was increasing for a consecutive 30 days at a low flow rate, but at 90 days it declined. As the day progresses, the values for the maximum value decrease.

4. Conclusion

Water samples were gotten analytically from the River Ikpoba in order to have a broad-spectrum overview of the water attribute state of the river. The outcomes of the analysis display a wide variation in the concentration of water quality parameters for both the rainy and dry seasons. PC1, PC2, PC3, PC4, PC5, PC6, and PC7 were influenced by high levels of heavy metals caused by geogenic industrial, atmospheric, farming and agrarian, pharmaceutical, and household effluents. Comparing investigation results with the current scenario around River Ikpoba, it is obvious that laboratory investigation imitates true pictures of effects around the river where most calamitous effects such as industrial effluence, religious deeds, flooding, drainage, riparian activities, fresh water matrices, and etcetera are triggered.

5. Declarations

5.1. Author Contributions

Conceptualization, L.O.A. and E.C.I.; methodology, L.O.A. and E.C.I.; software, L.O.A. and B.D.A.; validation, L.O.A., B.D.A., N.I.I. and E.C.I.; formal analysis, B.D.A. and N.I.I.; investigation, B.D.A. and N.I.I.; resources, N.I.I. and B.D.A.; data curation, L.O.A.; writing—original draft preparation, L.O.A.; writing—review and editing, E.C.I.; visualization, E.C.I.; supervision, N.I.I. and B.O.A.; project administration, N.I.I. and B.D.A.; funding acquisition, L.O.A., B.D.A., N.I.I. and E.C.I. All authors have read and agreed to the published version of the manuscript.

5.2. Data Availability Statement

The data presented in this study are available in the article.

5.3. Funding

The authors received no financial support for the research, authorship, and/or publication of this article.

5.4. Acknowledgements

Authors are grateful to the Water and Environmental Engineering Laboratory, Department of Civil Engineering University of Benin, Edo State Nigeria, for conductive environmental and assistance rendered during the field survey and experimental.

5.5. Institutional Review Board Statement

Not applicable.

5.6. Informed Consent Statement

Not applicable.

5.7. Declaration of Competing Interest

The authors declare that there is no conflict of interests regarding the publication of this manuscript. In addition, the ethical issues, including plagiarism, informed consent, misconduct, data fabrication and/or falsification, double publication and/or submission, and redundancies have been completely observed by the authors.

6. References

[1] Ciupak, M., Ozga-zieliński, B., Tokarczyk, T., & Adamowski, J. (2021). A probabilistic model for maximum rainfall frequency analysis. Water (Switzerland), 13(19), 2688–2695. doi:10.3390/w13192688.

[2] Yuan, J., Emura, K., Farnham, C., & Alam, M. A. (2018). Frequency analysis of annual maximum hourly precipitation and determination of best fit probability distribution for regions in Japan. Urban Climate, 24, 276–286. doi:10.1016/j.uclim.2017.07.008.

[3] Igibah, E. C., Agashua, L. O., & Sadiq, A. A. (2020). Hydro-geochemical features and groundwater attribute evaluation in North - central Abuja, Nigeria. Scientific African, 8, 10–21. doi:10.1016/j.sciaf.2020.e00324.

[4] Igibah, C. E., & Tanko, J. A. (2019). Assessment of urban groundwater quality using Piper trilinear and multivariate techniques: a case study in the Abuja, North-central, Nigeria. Environmental Systems Research, 8(1), 1–15. doi:10.1186/s40068-019-0140-6.

[5] Ogwueleka, T. C., & Christopher, I. E. (2020). Hydrochemical interfaces and spatial assessment of Usuma River water quality in North-Central Nigeria. Scientific African, 8, 1–18. doi:10.1016/j.sciaf.2020.e00371.

[6] Igibah, E. C., Amu, O. O., Agashua, L. O., & Adetayo, O. A. (2021). Hydro-geochemical autographs, attribute indicators and health threat evaluation of Fluoride and Ironic elements variability in ground water in Abuja North-central Nigeria. Fuel Communications, 10, 100048. doi:10.1016/j.jfueco.2021.100048.

[7] Amu, O. O., Amu, E. O., Igibah, E. C., & Agashua, L. O. (2021). Human health risk evaluation of sodium and ironic elements variability in ground water: A case study of Abuja North, Nigeria. Fuel Communications, 10, 100041. doi:10.1016/j.jfueco.2021.100041.

[8] Ablain, M., Jugier, R., Marti, F., Dibarboure, G., Couhert, A., Meyssignac, B., & Cazenave, A. (2020). Benefit of a second calibration phase to estimate the relative global and regional mean sea level drifts between Jason-3 and Sentinel-6a. Earth and Space Science Open Archive, 1, 1–10. doi:10.1002/essoar.10502856.2.

[9] Aura, C. M., Nyamweya, C. S., Owili, M., Gichuru, N., Kundu, R., Njiru, J. M., & Ntiba, M. J. (2020). Checking the pulse of the major commercial fisheries of Lake Victoria Kenya, for sustainable management. Fisheries Management and Ecology, 27(4), 314–324. doi:10.1111/fme.12414.

[10] Ablain, M., Meyssignac, B., Zawadzki, L., Jugier, R., Ribes, A., Spada, G., Benveniste, J., Cazenave, A., & Picot, N. (2019). Uncertainty in satellite estimates of global mean sea-level changes, trend and acceleration. Earth System Science Data, 11(3), 1189–1202. doi:10.5194/essd-11-1189-2019.

[11] Okonofua, E. S., Nwadialo, I. B., & Ekun, M. O. (2019). Modelling Ikpoba River Water Quality Using Principal Component Analysis (Pca) Method. Journal of Civil Engineering, Science and Technology, 10(1), 59–74. doi:10.33736/jcest.1083.2019.

[12] Dunn, R., Lief, C., Peng, G., Wright, W., Baddour, O., Donat, M., Dubuisson, B., Legeais, J. F., Siegmund, P., Silveira, R., Wang, X. L., & Ziese, M. (2021). Stewardship maturity assessment tools for modernization of climate data management. Data Science Journal, 20(1), 1–20. doi:10.5334/dsj-2021-007.

[13] Bonnefond, P., Exertier, P., Laurain, O., Guinle, T., & Féménias, P. (2021). Corsica: A 20-Yr multi-mission absolute altimeter calibration site. Advances in Space Research, 68(2), 1171–1186. doi:10.1016/j.asr.2019.09.049.

[14] Couhert, A., Mercier, F., Moyard, J., & Biancale, R. (2018). Systematic Error Mitigation in DORIS-Derived Geocenter Motion. Journal of Geophysical Research: Solid Earth, 123(11), 10,142-10,161. doi:10.1029/2018JB015453.

[15] Fasullo, J. T., & Nerem, R. S. (2018). Altimeter-era emergence of the patterns of forced sea-level rise in climate models and implications for the future. Proceedings of the National Academy of Sciences of the United States of America, 115(51), 12944–12949. doi:10.1073/pnas.1813233115.

[16] Ilaboya, I. R., Oti, E. O., Ekoh, G. O., Umukoro, L. O., & Enamuotor, B. O. (2014). Assessment of water quality index of some selected boreholes around dump sites in Nigeria. International Journal of Environmental Monitoring and Protection, 1(2), 47-55.

[17] Maghsood, F. F., Moradi, H., Bavani, A. R. M., Panahi, M., Berndtsson, R., & Hashemi, H. (2019). Climate change impact on flood frequency and source area in northern Iran under CMIP5 scenarios. Water (Switzerland), 11(2), 1–21. doi:10.3390/w11020273.

[18] Benka-Coker, M. O., & Ojior, O. O. (1995). Effect of slaughterhouse wastes on the water quality of Ikpoba River, Nigeria. Bioresource Technology, 52(1), 5–12. doi:10.1016/0960-8524(94)00139-r.

[19] Melet, A., Buontempo, C., Mattiuzzi, M., Salamon, P., Bahurel, P., Breyiannis, G., Burgess, S., Crosnier, L., Le Traon, P. Y., Mentaschi, L., Nicolas, J., Solari, L., Vamborg, F., & Voukouvalas, E. (2021). European Copernicus Services to Inform on Sea-Level Rise Adaptation: Current Status and Perspectives. Frontiers in Marine Science, 8, 1–8. doi:10.3389/fmars.2021.703425.

[20] Legeais, J. F., Ablain, M., Zawadzki, L., Zuo, H., Johannessen, J. A., Scharffenberg, M. G., Fenoglio-Marc, L., Joana Fernandes, M., Baltazar Andersen, O., Rudenko, S., Cipollini, P., Quartly, G. D., Passaro, M., Cazenave, A., & Benveniste, J. (2018). An improved and homogeneous altimeter sea level record from the ESA Climate Change Initiative. Earth System Science Data, 10(1), 281–301. doi:10.5194/essd-10-281-2018.

[21] Loeb, N. G., Thorsen, T. J., Norris, J. R., Wang, H., & Su, W. (2018). Changes in Earth's energy budget during and after the "Pause" in global warming: An observational perspective. Climate, 6(3), 62–74. doi:10.3390/cli6030062.

[22] Ekhaise, F. O., & Anyasi, C. C. (2005). Influence of breweries effluent discharge on the microbiological and physicochemical quality of Ikpoba River, Nigeria. African Journal of Biotechnology, 4(10). 1062–1065.

[23] USEPA. (2009). Impervious Cover, Ecosystems Research Division.U.S. Environmental Protection Agency, Athens, Georgia, United States.

[24] Haghighi, A.T., & Kløve, B. (2015). Development of monthly optimal flow regimes for allocated environmental flow considering natural flow regimes and several surface water protection targets. Ecological Engineering, 82, 390–399. doi:10.1016/j.ecoleng.2015.05.035.

[25] Mertikas, S. P., Donlon, C., Féménias, P., Mavrocordatos, C., Galanakis, D., Tripolitsiotis, A., Frantzis, X., Tziavos, I. N., Vergos, G., & Guinle, T. (2018). Fifteen years of Cal/Val service to reference altimetry missions: Calibration of satellite altimetry at the permanent facilities in Gavdos and Crete, Greece. Remote Sensing, 10(10), 1557–1566. doi:10.3390/rs10101557.

[26] Richter, B. D., Benoit, K., Dugan, J., Getacho, G., LaRoe, N., Moro, B., … Townsend, A. (2020). Decoupling Urban Water Use and Growth in Response to Water Scarcity. Water, 12(10), 2868. doi:10.3390/w12102868

[27] IPCC. (2022). The Ocean and Cryosphere in a Changing Climate. (Eds.)H.O. Pörtner, D. C. Roberts, V. Masson-Delmotte, P. Zhai, M. Tignor, & E., The Ocean and Cryosphere in a Changing Climate. IPCC. doi:10.1017/9781009157964.